

Development and Validation of an Aero-engine Simulation Model for Advanced Controller Design

Sonny Martin, Iain Wallace and Declan G. Bates

Abstract—This paper reports the results of a joint academic and industrial study on the development of a detailed simulation model to be used for research into advanced control strategies for civil turbofan aircraft engines. A comprehensive nonlinear dynamic model of a turbofan jet engine has been developed and validated against real industrial data. A switched, gain-scheduled, feedback control system incorporating bumpless transfer and antiwindup functionality has been designed for the engine model and implemented according to current industrial practice. Full flight envelope validation of the model has been performed with the help of Alstom Aerospace by analysing the resulting closed-loop performance properties for a range of different pilot thrust demands against the type of responses required from a real turbofan engine. In this paper, we present a detailed description of the modeling process, the various simulation issues that arise with a model of this complexity, and the validation results of the overall aero-engine system.

I. INTRODUCTION

In this paper we present a full aero-thermodynamic modular model of a 2-spool, high-bypass turbofan engine with an unmixed exhaust together with a switched, gain-scheduled aero-engine controller with bumpless transfer and antiwindup. Model implementation is in the Matlab-Simulink[®] environment. Full flight-envelope validation of both the model and controller has been performed with the assistance of Alstom Aerospace, with the exception of engine start-up as this is outside the boundary of validity of this model. The model is also compatible with the Real-Time-Workshop, a toolbox available in the Matlab-Simulink environment that is able to automatically generate a source code in C language from the Simulink scheme. This feature can be useful for developing a code for hardware-in-the-loop applications. The purpose of the model is the development of advanced control strategies, therefore a baseline controller that closely mirrors industrial practice is included in the model. The controller has also a modular approach, allowing easy extension to the parameters regulated by the controller. The model is provided with a 'dashboard' that allows realtime inspection of significant parameters such as massflow, temperature and pressure at each engine station.

There are relatively few papers in the literature that deal specifically with civil aircraft engines. Several papers provide an architecture for simulating gas turbines [1] [2] [3] [4] [5] [6] [7] [8], but most are applied to industrial turbines and few provide details of implementations suitable for civil aircraft engines [9]. This paper includes additional details specific to civil aircraft engines: the fan of the engine (this absorbs a significant proportion of the power output by the engine and an accurate model is highly desirable) is modeled as two separate sections, a core section and a duct section, with therefore different pressure ratio and efficiency as would be the case for a real engine. A nozzle module suitable for an aerothermal model (i.e. that does not require iterative procedures) and a model of the duct (as a nozzle) are also provided, so that fan power consumption

may be accurately calculated. Transfer of heat to and from the engine components is also taken into consideration by providing heat storage modules for each major component because heat soak can have a significant effect upon the dynamics of the engine, particularly at high altitude where the massflow through the engine is greatly reduced. Indeed the range of environmental and operating conditions that an aero-engine can be expected to undergo is much greater than those of industrial engines. An aero-engine must be able to perform to stringent requirements under dramatically varying environmental conditions and very different regimes e.g. rapid acceleration/deceleration, take off and idle. For validation of the model under these varying conditions a gain-scheduled controller is provided.

The paper is structured as follows: first is provided a brief introduction to the main components of a civil turbofan aero-engine, then selected simulation details are presented in Section II, followed by an overview of implementation issues in Section III. Section IV discusses the validation and performance results of the simulation.

II. MODULAR CONSTRUCTION OF THE MATHEMATICAL MODEL

A. Model Overview

The type of engine considered is the separated flow turbofan. This has been found to be the optimum configuration for high subsonic commercial aircraft [10]. A turbofan's airflow is split into two main sections, as shown in fig. 1. The outer 'duct' or 'bypass' airflow is accelerated by a fan situated at the front of the engine. This section provides most of the engine's thrust by moving a large mass of air at a relatively low speed. The inner or 'core' section provides the power to drive the fan. Airflow through this section is compressed via two sequential compressors: a low pressure (LP) compressor and a high pressure (HP) compressor. The high pressure flow at the exit of the high pressure compressor is in part combusted then the hot flow expands through the HP turbine (this powers the HP compressor), and then flows into the LP turbine (this powers the LP compressor and the fan). A further expansion to atmospheric pressure is via a fixed convergent nozzle placed at the rear of the LP turbine. The shaft connecting the fan, LP compressor and LP turbine is called the 'low pressure shaft', and similarly the shaft connecting the HP compressor and the HP turbine is known as the 'high pressure shaft'. These two shafts are concentric: the LP shaft extends beyond and rotates within the HP shaft. Fig. 1 outlines how these turbofan components are interconnected. The variable bleed valve placed between the LPC and the HPC improves the surge characteristics [5] [7] by purging air directly into the duct (surge is a violent oscillatory reversal of the gas stream's flow). For the same reason the HPC module is provided with a model of variable stator vanes (VSVs). The operation of both these components is open loop scheduled with corrected shaft speed. The simulation uses 'lumped' elements: the engine components are simplified to volume-less elements, thereby reducing the partial differential equations that describe their distributed properties to ordinary differential equations that describe the evolution of key properties over time. The unsteady mass balance between components is modeled via

Grateful acknowledgment goes to Alstom Aerospace and the UK Engineering and Physical Sciences Research Council for financial support via a CASE studentship award.

S. Martin and D.G. Bates are with the Control and Instrumentation Research Group, Department of Engineering, University of Leicester, UK sm342, dgb3@le.ac.uk

I. Wallace is with Alstom Aerospace, Cambridge Road, LE8 6LH Whetstone, UK

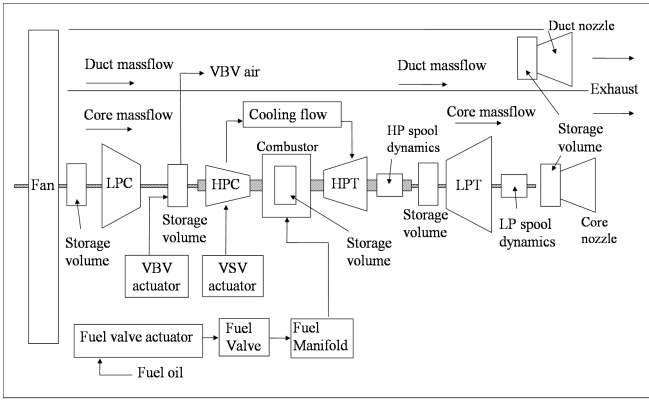


Fig. 1. The main components of a turbofan engine

storage volumes (plenums). The aim is to derive a set of explicit, first order differential equations which can be solved using an integration algorithm to accurately describe the dynamic characteristics of the modeled components. Once atmospheric conditions, namely altitude, Mach Number, temperature deviation from the International Standard Atmosphere (ISA), and the value of the control variables, e.g. fuel flow and other control parameters that are open loop scheduled (e.g. bleed valve position) have been specified then the operating point follows via a feed-forward calculation that propagates along the engine's direction of flow. A few notable exceptions are addressed via use of Simulink 'memory blocks' (see section III) - this is so that thermodynamic properties can be based on a component's mean temperature and the compressors can be provided with pressure data from downstream components. The stagnation conditions at the engine inlet are computed with Saint-Venant-Wantzel relations [10] as a function of altitude, variation from ISA day temperature and Mach Number. This accounts for ram recovery at the engine's inlet.

B. Component Models

Each modular component can be viewed as an operator the purpose of which is to compute the thermodynamic state of the fluid (typically mass flow \dot{w} , total temperature and pressure) at the outlet of the module based on the inlet conditions and some additional parameters. Each component model relies on the equations for mass, momentum and energy balances and on empirical information derived from rig tests or advanced CFD calculations, e.g. compressor and turbine characteristic maps. The thermodynamic properties of the air stream and combustion gases will vary due to the range of environmental and operating conditions at which the engine must operate. This makes an accurate evaluation of the gas stream's thermodynamic properties highly desirable for an aero-engine. Lookup tables may be used (tables containing the values of the specific heats have been published in many references [11] [6]) or, as in the present case, algebraic curve-fitting expressions [12] may be used. Therefore in the present work the working fluids are not considered as perfect gases of constant specific heats, as this is mainly appropriate for preliminary design calculations [10]. This has the advantage of both improved accuracy and preserves a computational architecture that allows for complex scenarios to be simulated e.g. ingestion of water vapour and dramatic changes in inlet temperature. The specific heat at constant pressure, c_p , was provided by the polynomial fits in [12] and is temperature and fuel-air-ratio (FAR) dependent. The gas constant, R , is temperature independent and FAR dependent. The ratio of specific heats, γ , is temperature and FAR dependent and

can be expressed as a function of the specific heat capacity, c_p , and the gas constant R . It should be noted that for formulae using c_p and γ it is most accurate to base these values on the mean temperature for each component, i.e. the arithmetic mean of the inlet and outlet values. It is less accurate to evaluate c_p and γ at inlet and outlet, and then take a mean value for each [12].

C. Plenums

Because turbomachinery, compressor and turbine units are considered as volume-less elements, a plenum is placed at the compressor outlet in order to take into account the unsteady mass balance at compressor discharge, within the combustion chamber, and between the turbines and the low pressure turbine and the nozzle. Mass conservation implies:

$$\dot{w} = \int (\dot{w}_{in} - \dot{w}_{out}) \cdot dt + w_0, \quad (1)$$

where w is the mass present in the casing, \dot{w} represents gas stream mass flow [$kg \cdot s^{-1}$] and w_0 is the initial value of the mass present in the plenum. Pressure inside the plenum is then calculated via the ideal gas law:

$$p_{out} = w \cdot \frac{T \cdot \bar{R}}{V}, \quad (2)$$

where \bar{R} is the specific gas constant of the gas stream [$J \cdot kg^{-1} \cdot K^{-1}$]. Each plenum also includes a module to calculate the heat soak of the component upstream. If this was not included the plenum's outlet temperature would be equal to the inlet temperature. Energy accumulation due to transient effects such as volume packing [12] is neglected. Pressure losses are also not considered - these are easily implemented if desired [10] [13].

D. Heat Soakage

Each turbomachinery component includes heat transfer effects, such as the heat transfer to turbine blades and casings. Only convective heat transfer is considered based on simplified equations for turbulent flow over a flat plate and assuming a constant Prandtl number [14]. By considering a lump of metal (e.g. a blade) in a hot gas flow a simple, first order heat soak equation can be developed. The time constant, τ , can be calculated from the heat transfer coefficient and the mass and specific heat capacity of the metal. The heat transfer coefficient is calculated for the design point conditions and modified at off-design conditions depending on mass flow and temperature which both alter the flow's Reynold number. It has been demonstrated that heat soak effects play an important part in determining a gas turbine's dynamic performance [15], yet they are extremely difficult to predict in the absence of good test data. In the absence of such data, the heat soak released upon an abrupt deceleration of an industrial engine [16] was scaled down for the current model. The time constant was similarly reduced. The overall heat soak quantity was then distributed amongst the components according to their mass and the temperatures reached. Key equations for the implementation of a heatsoak module follow. The most fundamental equation is Newton's law of cooling:

$$q = \bar{h}A \cdot \Delta T = \bar{h}A (T_m - \bar{T}), \quad (3)$$

where q is the heat flow [W], \bar{h} is the average heat transfer coefficient over the surface [$Wm^{-2}K^{-1}$], T_m is the component average temperature, \bar{T} is the gas stream's mean temperature and A is the heat transfer area [m^2]. The heat transfer coefficient is temperature and flow dependent, and this dependency can be approximated with the following relationship [17]:

$$Y \propto T^{0.23} \cdot \dot{w}^{0.8}, \quad (4)$$

where \dot{w} is mass flow rate and

$$Y = \bar{h}A \quad (5)$$

In experimental conditions the easiest parameter to measure will be the time constant τ . This can be obtained by rapidly increasing or decreasing the gas stream temperature from a starting condition with the gas and metal mass in thermodynamic equilibrium at a known temperature:

$$\frac{dT_m}{dt} = -\frac{q}{Mc_{pm}}, \quad (6)$$

where T_m is the metal temperature, M is the metal mass and c_{pm} is the metal specific heat capacity. The two equations (6) and (3) above can be combined to give:

$$\frac{dT_m}{dt} = -\frac{\bar{h}A(T_m - \bar{T})}{Mc_{pm}} \quad (7)$$

Since the time constant is

$$\tau = \frac{Mc_{pm}}{\bar{h}A}, \quad (8)$$

then it follows that

$$\frac{dT_m}{dt} = -\frac{1}{\tau} \Delta T \quad (9)$$

Therefore the time constant of the system can be experimentally determined. Once this is known, for a system of similar mass and area the following equations can be applied:

$$Y_d = \bar{h}A = \frac{1}{\tau_d} Mc_{pm}, \quad (10)$$

where Y_d is the value of Y established under the experimental conditions T_d , \dot{w}_d , and τ_d . From this it follows that:

$$\begin{aligned} q &= Y \cdot \Delta T = \Delta T \cdot Y_d \cdot \frac{\tau_d}{\tau} = \Delta T \cdot Y_d \cdot \left(\frac{\tau}{\tau_d}\right)^{-1} \\ &= \Delta T \cdot Y_d \cdot \left[\left(\frac{\bar{T}}{T_d}\right)^{-0.23} \left(\frac{\dot{w}}{\dot{w}_d}\right)^{-0.8} \right]^{-1} \end{aligned} \quad (11)$$

This is because:

$$\tau = \tau_d \left[\left(\frac{\bar{T}}{T_d}\right)^{-0.23} \left(\frac{\dot{w}}{\dot{w}_d}\right)^{-0.8} \right] \quad (12)$$

This last relationship follows from the considerations given below.

$$\tau = \frac{Mc_{pm}}{\bar{h}A} \approx \frac{k}{\bar{h}} \quad (13)$$

where k is a constant. From (4):

$$\bar{h} \approx k_1 \cdot T_d^A \cdot \dot{w}_d^B \quad (14)$$

It then follows that:

$$\tau_d = \left(\frac{k}{k_1}\right) \cdot T_d^{-A} \cdot \dot{w}_d^{-B} = k_d^* \cdot T_d^{-A} \cdot \dot{w}_d^{-B} \quad (15)$$

Considering a new time constant τ at different temperature and massflow conditions:

$$\tau = k^* \cdot T^{-A} \cdot \dot{w}^{-B}, \quad (16)$$

and therefore:

$$\frac{\tau}{\tau_d} = \frac{k^* \cdot T^{-A} \cdot \dot{w}^{-B}}{k_d^* \cdot T_d^{-A} \cdot \dot{w}_d^{-B}} \quad (17)$$

and if

$$k_d^* = k^*, \quad (18)$$

which holds for components of similar geometries [14], then:

$$\frac{\tau}{\tau_d} = \frac{T^{-A} \cdot \dot{w}^{-B}}{T_d^{-A} \cdot \dot{w}_d^{-B}} = \left(\frac{T}{T_d}\right)^{-A} \left(\frac{\dot{w}}{\dot{w}_d}\right)^{-B} \quad (19)$$

Therefore if Y_d and τ_d have been established experimentally then the formula (11) can be applied to get the heat transferred q [W], over a range of temperatures and massflows. This heat can then be directly added or subtracted to the enthalpy of the gas stream.

E. Fan and Compressors

The fan placed at the front of the turbofan provides the majority of the engine's thrust. The fan simulation module is divided into two sections: a core and a duct section. The ratio between the duct and core massflows is known as the bypass ratio (BPR):

$$BPR = \frac{\dot{w}_{duct}}{\dot{w}_{core}} \quad (20)$$

Each section is modeled via a characteristic map, describing the steady state performance of the component. The performance can be specified by curves of delivery pressure and temperature plotted against mass flow for various fixed values of rotational speed. These characteristic curves are however dependent upon other variables such as the conditions of pressure and temperature at entry and the physical properties of the working fluid. By using dimensional analysis the variables involved may be combined to form a smaller and more manageable number of dimensionless groups and these characteristic curves can then be plotted on a non-dimensional basis, i.e. stagnation pressure ratio and isentropic efficiency η_i against the non-dimensional mass flow rate \dot{w} for fixed values of the non-dimensional speed $(n/\sqrt{\theta})$ [12]. The fan's corrected massflow is provided by the characteristic map once the fan's pressure ratio and corrected shaft speed have been provided. Applying the conservation equations the temperature increase over the fan is described by:

$$T_{out} = T_{in} \cdot \left[1 + \frac{1}{\eta_i} \cdot \left(\pi^{\frac{\gamma-1}{\gamma}} - 1 \right) \right], \quad (21)$$

where π is the pressure ratio over the core or duct section of the fan, γ is the ratio of specific heats and η_i is the isentropic efficiency. The power required to drive the fan is then:

$$P_{fan} = c_p \cdot \dot{w} \cdot (T_{out} - T_{in}) \quad (22)$$

and is positive since it is supplied to the air.

The air that flows through the core section of the engine is compressed via two compressors in series. These are modeled in a similar fashion to the fan, except that there is no splitting of the mass flow. Characteristic maps are again at the core of the compressor models and the constitutive equations are the same. More complex models would split the compressor into stages separated by small plenums and solve gas flow equations based on a knowledge of blade angle and stage performance but the approach adopted is more practical, particularly for a generic turbofan model where data requirements are not too onerous [18].

Between the two compressors there is an open loop scheduled bleed valve (VBV). This extracts air from the core flow and exhausts directly into the duct. The percentage

of massflow extracted is scheduled with the corrected LP shaft speed. For predicted effect of VBV's see [7]. The second of the compressors in series, the high pressure compressor (HPC) also includes bleeds (these power aircraft accessories) and variable stator vanes (VSVs). The latter are to improve the surge margin of the HPC and are modeled by a percentage reduction in corrected mass flow. This reduction is open loop scheduled against corrected HP shaft speed. See [7] for plots of the effects of VSVs on compressor maps. The bleeds are modeled by extracting a percentage of the inlet air flow. This air will not be available for work in the compressor and this is reflected in the formula for HPC power:

$$\begin{aligned} \text{HPC}_{power} &= \\ &= c_p \cdot \dot{w} \cdot (T_{out} - T_{in}) \cdot [k_1 x_1 + k_2 x_2 + (1 - k_1 - k_2)] \quad (23) \end{aligned}$$

where k_1 and k_2 are the proportion of air removed via bleeds 1 and 2 respectively and x_1 and x_2 are scalars from 0 to 1 that represent the proportion of the total temperature rise to be expected at that stage. Cooling air is extracted prior to the combustor, at the outlet of the HPC. Cooling flow is an important element of the model because the total percentage of engine inlet mass flow extracted before the combustor may be up to 25% for a high technology aero or industrial engine [12], and cooling flow will represent a significant proportion of this. Cooling flow is often modeled simply as a percentage of the engine's massflow [10] but in this case it was preferred to use a relation that, although empirical, is based on the ratio of the pressure of the air source (the HPC) and that of the sink (the HPT) [4] [19]:

$$\dot{w}_{cool} = K \cdot \sqrt{1 - \frac{p'_{out}}{p_{in}}} \cdot \frac{p_{in}}{\sqrt{T_{in}}} \quad (24)$$

where K is a discharge coefficient, p_{in} and T_{in} are respectively the pressure and temperature at the bleed point and p'_{out} is the static pressure at the exit of the cooling circuit. In this work this is approximated by the pressure value at the cooling flow exit. This is reasonable since the velocity of the gas stream is relatively low at this stage and dynamic pressure remains a low proportion of the total up to approximately Mach 0.4 [12].

F. Combustor

The air at the outlet of the HPC is passed into a combustion chamber. This increases the enthalpy of the working fluid via the combustion of fuel. The flame temperatures in the model are obtained from 2-D lookup tables that were calculated using NASA program SP273. This data was extracted from [20]. Therefore the exit temperature of the combustor is provided as a function of excess air factor, λ , and inlet temperature. To account for the unsteady mass balance between the HPC, combustor and HPT a storage volume is included in the combustor.

G. Turbines

The hot gas stream exits the combustor and is expanded via two turbines in series. Again, a characteristic map is used to represent each turbine. The constitutive equation for the temperature drop across the turbine is:

$$T_{inlet} - T_{outlet} = \eta_t \cdot T_{in} \left[1 - \left(\frac{1}{p_{in}/p_{out}} \right)^{\frac{\gamma-1}{\gamma}} \right] \quad (25)$$

where η_t is the turbine isentropic efficiency. The HPT, although not modeled as a multi-stage cooled turbine, does include injection of cooling air from the HPC. Cooling air is injected into the main stream at the turbine inlet, therefore

a mixing procedure has to be included in the module. For calculations of work the whole flow is used i.e. both the hot gases and the cooling air do work in the turbine. The mixing block takes the mass fraction of cooling air and calculates the temperature of the mixed flow:

$$T_{mix} = \frac{x \cdot T_{cool} \cdot c_{p,cool} + (1-x) \cdot T_{inlet} \cdot c_{p,hot}}{x \cdot c_{p,cool} + (1-x) \cdot c_{p,hot}}, \quad (26)$$

where x is the mass fraction of cooling air. The temperature of the mixture of hot and cold gas, T_{mix} , is then substituted for T_{inlet} in (25).

H. Exhaust System

Exhaust air exits the turbofan engine in two separate unmixed streams: duct air and core section air. Both the duct and core exhaust are modeled as convergent nozzles, each of a fixed area. A turbofan's core nozzle can be assumed to be unchoked over the operating range of the engine. The duct nozzle, due to the inherently low speed of the duct gas stream is also unchoked. Conditions at the inlet of the nozzle shall be denoted with subscript '0', e.g. p_0, v_0, T_0 for the pressure, specific volume and temperature respectively. Similarly conditions at the exit of the nozzle are denoted with subscript '1'. Conditions at the nozzle throat are denoted with subscript 't'.

The nozzles of a gas turbine receive a gas that already possesses an appreciable velocity, therefore the equations used to model the nozzle must incorporate factors to account for these significant inlet velocities. For a frictionally resisted, adiabatic expansion:

$$pv^m = constant, \quad (27)$$

where the polytropic exponent, m , is a function of the adiabatic index, γ , and nozzle efficiency η_N :

$$m = \frac{\gamma}{\gamma - \eta_N(\gamma - 1)} \quad (28)$$

The nozzle throat will pass flow at speeds up to and including sonic but cannot support supersonic flow (a convergent nozzle slows down supersonic fluids). Sonic flow will be reached when the ratio of throat pressure p_t to inlet stagnation pressure p_0 has reached a critical value (the nozzle is 'choked'):

$$\frac{p_{tc}}{p_{0T}} = \left(\frac{2}{\gamma + 1} \right)^{\frac{m_c}{(\gamma - 1)}}, \quad (29)$$

where p_{tc} and m_c are respectively the throat pressure and polytropic exponent at these critical conditions.

The non-negligible gas velocity may be accounted for by using the concepts of stagnation pressure, p_{0T} , and stagnation temperature, T_{0T} . Furthermore, assuming that nozzle efficiency is constant over the length of the nozzle (the variation, for a convergent only nozzle, has been found in practice to be small up to and including sonic velocity [21]) and under the assumption that pressure and specific volume in the stagnation state are related to temperature by:

$$p_{0T} v_{0T} = \bar{R} T_{0T}, \quad (30)$$

where \bar{R} is the specific gas constant, the nozzle's massflow is then:

$$\dot{w} = A \sqrt{2 \frac{\gamma}{\gamma - 1} \frac{p_{0T}}{v_{0T}} \left(\left(\frac{p_1}{p_{0T}} \right)^{\frac{2}{m_0}} - \left(\frac{p_1}{p_{0T}} \right)^{\frac{(m_0+1)}{m_0}} \right)} \quad (31)$$

for

$$\frac{p_1}{p_{0T}} \geq \left(\frac{2}{\gamma + 1} \right)^{\frac{m_c}{(\gamma - 1)}}, \quad (32)$$

i.e. for subsonic flow. A is the throat area and is the same as the exit area for a convergent-only nozzle. An important issue is that there is no value for the specific volume at stagnation conditions, v_{0T} , in the model at this stage, but this can easily be calculated from the relationship in (30).

I. Shafts

Speeds at time t are calculated using unbalanced powers, speeds from the previous point and the spool inertias. The rotational acceleration of the shaft can be found from the shaft dynamic balance: For example, for the LP shaft:

$$\frac{d\omega}{dt} = \frac{1}{I\omega} (P_{HPT} - P_{LPC} - P_{Fan} - P_{losses}) \quad (33)$$

where P is power, I is shaft moment of inertia and ω is the shaft angular speed. Power losses are caused by friction and engine accessories and can be modeled as a simple percentage of the total power provided to the shaft, or as a loss that is proportional to shaft speed.

J. Actuators

Models for mechanical actuators such as those of the fuel system valve, the variable bleed valves and the stator vanes are also included. These are modeled in terms of first and second order Laplace transforms (transfer functions) [5]. The temperature sensor (transducer), also has its own dynamics and these too are represented in the model via transfer functions according to the representation in [22].

III. SIMULATION ISSUES

A. Model Initialisation

The model has been developed for the purpose of investigating advanced strategies for robust fault tolerant aero-engine control. Clearly it is of great benefit to provide an implementation architecture that allows for rapid alteration of the model to simulate faults and adaptation to different engine configurations if so wished. One way of doing this is to initialise as much of the model as possible from scripts. For example, all Simulink tables where possible are initialised using workspace vectors. Scripts can assign upon intialisation values to all lookup tables, enabling the model to be rapidly changed if required. In the same way, major parameters can be made time dependent if their values are provided via 'from workspace' blocks. For the same reason the scaling of each characteristic map is performed online as the model runs, with each of the scaling parameters provided by workspace variables.

B. Algebraic Loops

Algebraic loops occur if a module requires data from elements downstream. This is a major issue for the compressors and turbines because outlet pressure data is required to calculate the pressure ratio across the component and thus, via the characteristic map, the component's massflow. It is also good practice to calculate thermodynamic parameters based on a component's average temperature (see section II) but this requires knowledge of the component's outlet temperature prior to its calculation by the simulation module. If these algebraic loops are not specifically eliminated the Simulink loop solver uses Newton's method to iteratively find a solution [23]. Although the method is robust, it is possible to create loops for which the loop solver will not converge without a good initial guess for the algebraic states. An alternative method that is particularly advantageous for the current model is to specify a one-time-step delay by using a 'memory' block, thereby avoiding the need for iterative calculations that would slow down the simulation considerably. This is made possible by means of the approximations that are applicable to real-time gas turbine dynamic models in consideration of the very short time step used in the simulation.

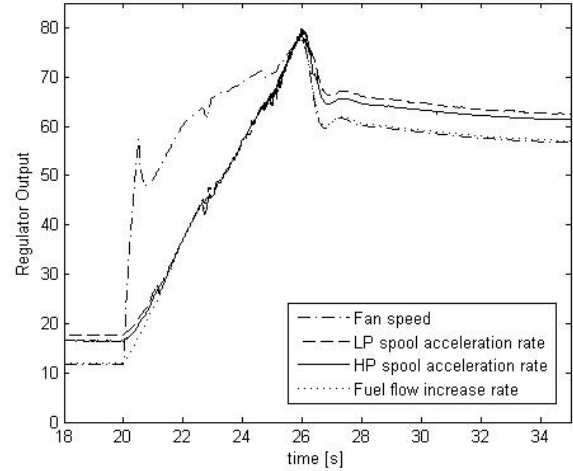


Fig. 2. Active regulators' output during acceleration.

IV. CLOSED LOOP PERFORMANCE VALIDATION

Several methods of gas turbine simulation dynamic performance validation have been used in the past, e.g. [9] uses GasTurb [13], a commercial software dedicated to gas turbine modeling and [1] matches calculated performance to previously published results [5].

The current model and controller have been validated against dynamic performance data for a comparable engine by analysing the resulting closed-loop performance properties for a range of different pilot thrust demands against the type of responses required from a real turbofan engine. Further details of the controller implemented can be found in [24]. Some snapshots of the overall performance of the model and controller can be seen in the following plots. Although the model as developed is non-proprietary, some specific performance figures of this configuration have on this occasion been omitted for reasons of commercial sensitivity. Fig. 2 shows the individual fuel demands of the active regulators during a pilot request - in this case an abrupt increase in thrust demand at Sea Level Static (SLS), to maximum thrust, in a time span of half a second. Fig. 3 shows the active regulators' demands during a deceleration. Fig. 4 shows the final controller demand after the controller's selection logic has been applied to the output of all regulators. By comparing this to figures 2 and 3, it is apparent that the controller has selected the smallest of the regulators' demands during acceleration, and that the transfer between these is smooth. Conversely it has selected the largest of the regulators' demands during deceleration. Note that the controller's output is converted to fuel flow units ($\text{kg}\cdot\text{s}^{-1}$) in a module external to the controller, to allow for an easy implementation of different fuels should the model be adapted in the future to a different configuration, e.g. an industrial aero-derivative engine. The overall controller output is a smooth ramp and engine acceleration proceeds accordingly until maximum thrust has been achieved. This is apparent in Fig. 5, which shows the engine's response to the pilot's demand: although the request is abrupt, the engine acceleration is smooth and at the maximum rate possible by running on the acceleration limits of its two shafts, subject to a maximum permissible rate of increase in fuel flow. Although this is not evident in the plot, there is a slight overshoot and undershoot of about 0.4%, but this is well within the FAA requirement of a deviation in thrust of not more than 2% [15], and can be reduced further, although at the cost of an increase in acceleration time.

V. CONCLUSIONS

This paper has presented details of the design and validation of a complex nonlinear realtime simulation model for a civil turbofan aircraft engine. The model was developed in a modular fashion using wherever possible the underlying physics and avoiding empirical approximations. A switched gain scheduled feedback controller incorporating bumpless transfer and antiwindup functionality was designed and implemented on the engine model in accordance with current industrial practice. Together the engine and controller cover the full flight envelope and achieve dynamic performance that closely matches that of a real engine. The control scheme corresponds closely to current industrial practice and delivers high-performance tracking of pilot demands while ensuring that the operating constraints of the engine are met at all times. Future work in this project will focus on extending the model to include various sources of uncertainty, fault and failure scenarios and extending the control scheme to deliver robust fault tolerant performance.

REFERENCES

- [1] S. M. Camporeale, B. Fortunato, and A. Dumas, "Dynamic modeling and control of regenerative gas turbines," *98-GT-172*, 1998.
- [2] S. M. Camporeale, M. Agresti, and B. Fortunato, "An object-oriented program for the dynamic simulation of gas turbines," *ASME 2000-GT-42*, 2000.
- [3] S. M. Camporeale, L. Dambrosio, and B. Fortunato, "One-step ahead adaptive control for gas turbine power plants," *Journal of Dynamic Systems, Measurement, and Control*, vol. 124, pp. 341 – 348, 2002.
- [4] S. M. Camporeale, B. Fortunato, and M. Mastrovito, "A modular code for real time dynamic simulation of gas turbines in simulink," *Transactions of the ASME*, vol. 128, pp. 506 – 514, 2006.
- [5] W. I. Rowen, "Simplified mathematical representations of heavy-duty gas turbines," *Transactions of the ASME Journal of Engineering for Power*, vol. 105, pp. 865 – 869, 1983.
- [6] Q. Z. Al-Hamdan and M. S. Y. Ebaid, "Modeling and simulation of a gas turbine engine for power generation," *Journal of Engineering for Gas Turbines and Power*, vol. 128, pp. 302–311, April 2006 2006.
- [7] J. H. Kim, T. Song, T. Kim, and S. Ro, "Model development and simulation of transient behavior of heavy duty gas turbines," *Journal of Engineering for Gas Turbines and Power*, vol. 123, pp. 589–594, 2001.
- [8] W. P. J. Visser, O. Kogenhop, and M. Oostveen, "A generic approach for gas turbine adaptive modeling," *Journal of Engineering for Gas Turbines and Power*, vol. 128, pp. 13 – 19, 2006.
- [9] S. Borguet, V. Kelner, and O. Leonard, "Cycle optimisation of a turbine engine: an approach based on genetic algorithms," University of Liege, Aerospace and Mechanical Engineering Department, Tech. Rep.
- [10] H. Saravanamuttoo, H. Cohen, and G. Rogers, *Gas Turbine Theory*, 4th ed. Longman, 1996.
- [11] R. D. Archer and M. Saarlans, *An Introduction to Aerospace Propulsion*. New Jersey: Prentice Hall, 1996.
- [12] P. Walsh and P. Fletcher, *Gas Turbine Performance*, 1st ed. Blackwell Science, 1998.
- [13] J. Kurzke, *GasTurb Software*.
- [14] J. Welty, E. Wicks, R. Wilson, and G. Rorrer, *Fundamentals of momentum, heat, and mass transfer*. John Wiley and Sons, 2001.
- [15] A. Kreiner and K. Lietzau, "The use of onboard real-time models for jet engine control," MTU Aero Engines, Germany, Tech. Rep., 2001.
- [16] A. W. Pike, "Development of the gtx100 gas turbine simulink dynamic model," Alstom, Tech. Rep., November 2000.
- [17] F. Incropera and D. Dewitt, *Fundamentals of Heat and Mass Transfer*. John Wiley and Sons, 1990.
- [18] B. E. Ricketts, "Modelling of a gas turbine: a precursor to adaptive control," *IEEE: Adaptive controllers in Practice (Colloquium)*, 1997 1997.
- [19] W. F. McGreehan and M. J. Schotsch, "Flow characteristics of long orifices with rotation and corner radiusing," *Journal of Turbomachinery*, vol. 110, pp. 213–217, 1998.
- [20] *Alstom GTX100 dynamic simulation program*, Alstom.
- [21] P. Thomas, *Simulation of Industrial Processes for Control Engineers*. Butter-Heinemann, 1999.
- [22] L. N. Hannett and A. Khan, "Combustion turbine dynamic model validation from tests," *IEEE transactions on Power Systems*, vol. 8, no. 1, pp. 152 – 158, 1993.
- [23] Mathworks, *Simulink Manual*, 2005.
- [24] S. Martin, I. Wallace, and D. G. Bates, "An industrially validated control scheme for a civil aircraft engine," in *IFAC World Congress, Seoul 2008*, submitted September 2007.

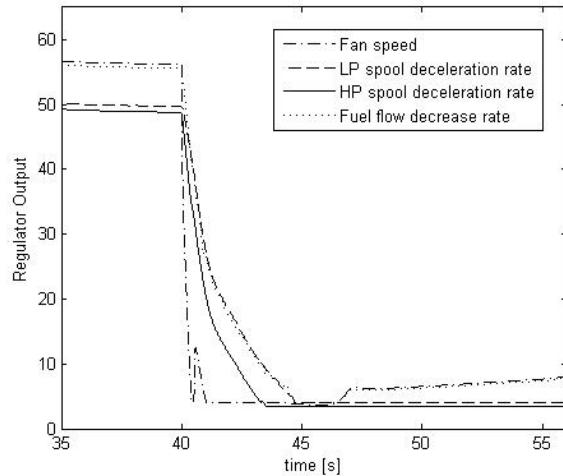


Fig. 3. Active regulators' output during deceleration.

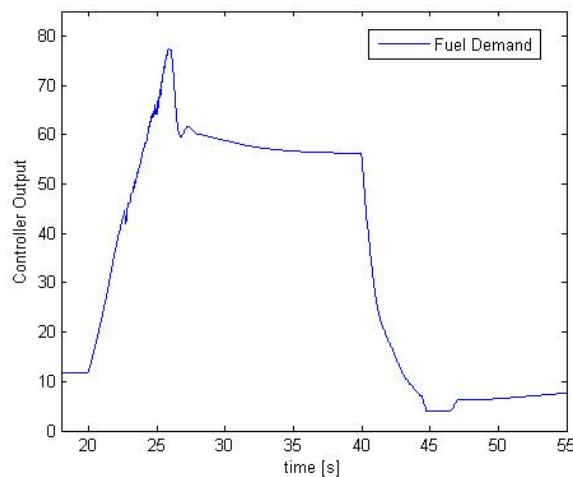


Fig. 4. Controller fuel demand.

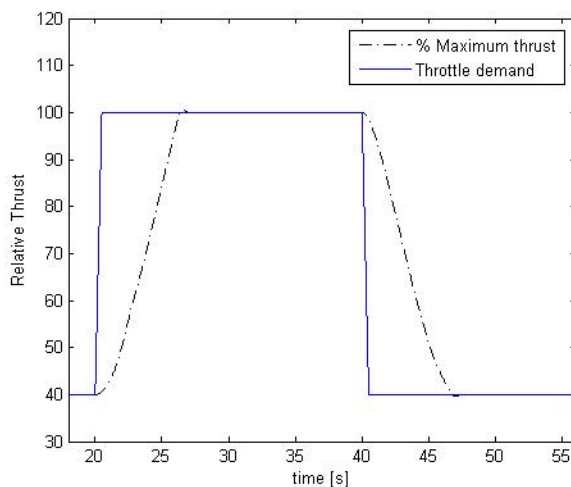


Fig. 5. Thrust response to large throttle demand